telecom

MDPI

Article

Binary Dragonfly Algorithm with Semicircular Mobility for Multi-Objective Optimization of Underwater Wireless Sensor Networks

Eduardo Vázquez, Aldo Mendez *, Leopoldo A. Garza, Alberto Reyna and Gerardo Romero

Electrical and Electronic Engineering Department, Universidad Autónoma de Tamaulipas, UAMRR-R, Carretera Reynosa-San Fernando, Reynosa 88779, Tamaulipas, Mexico; eduardovazquez271@gmail.com (E.V.); leopoldo.garza@docentes.uat.edu.mx (L.A.G.); alberto.reyna@docentes.uat.edu.mx (A.R.); gromero@docentes.uat.edu.mx (G.R.)

* Correspondence: almendez@docentes.uat.edu.mx; Tel.: +52-8999213300

Abstract

Underwater wireless sensor networks (UWSNs) support critical applications such as environmental monitoring, offshore exploration, and surveillance; however, their performance is constrained by high propagation delay, limited energy resources, and node mobility caused by ocean dynamics. Many clustering approaches assume static nodes and use fixed-weight objective aggregation, which may reduce adaptability and lead to premature convergence. This paper proposes a cluster-head selection and cluster formation method for UWSNs based on a binary multi-objective Dragonfly Algorithm (BMDA-UWSN). The method considers energy consumption, acoustic latency, and load balance within a Pareto-based optimization framework, thereby reducing dependence on fixed-weight aggregation during the search stage. In addition, the Dragonfly-based optimization process uses dynamically adjusted coefficients to regulate the balance between exploration and exploitation while preserving solution diversity. To represent underwater node displacement, a semicircular mobility model with angular variation of $\pm 45^{\circ}$ is incorporated into the simulation scenario. Results obtained for a 100-node network show that BMDA-UWSN achieved better performance than Direct Transmission, LEACH, LEACH-C, SS-GSO, and CDFO-UWSN in terms of network lifetime, packet delivery, latency, and residual energy under the evaluated conditions. In particular, the first node dies at iteration 126 with BMDA-UWSN, compared with iteration 95 for CDFO-UWSN, while packet delivery increases by approximately 20% and latency decreases by about 5%. These findings suggest that BMDA-UWSN is a competitive clustering approach for underwater monitoring scenarios when evaluated under controlled node mobility conditions.

Keywords: dragonfly algorithm; underwater wireless sensor networks; LEACH; firefly algorithm

Check for updates

Academic Editor: Achilles Boursianis

Received: 3 February 2026
Revised: 20 March 2026
Accepted: 7 April 2026
Published: 12 May 2026

Copyright: © 2026 by the authors. Licensee MDPI, Basel, Switzerland. This article is an open access article distributed under the terms and conditions of the Creative Commons Attribution (CC BY) license.

1. Introduction

Underwater wireless sensor networks (UWSNs) have enabled important applications such as environmental monitoring, ocean exploration, underwater observation, surveillance, and security operations [1]. Unlike terrestrial sensor networks, UWSNs primarily rely on acoustic communication, which severely constrains protocol design due to limited bandwidth, high propagation latency (≈1500 m/s), frequency-dependent absorption and scattering losses, strong spatiotemporal channel variability, multipath, and Doppler effects [2]. Furthermore, the difficulty of recharging or replacing batteries causes energy

limitations, which complicates network operation and protocol design. Furthermore, the difficulty of recharging or replacing batteries causes energy limitations, which complicates network operation and protocol design [3]. While numerous protocols have been proposed for terrestrial and ad hoc networks, underwater acoustic channels introduce unique challenges that require specially tailored solutions. Compared to terrestrial networks, UWSNs typically involve higher manufacturing and deployment costs, lower node density due to installation constraints, greater inter-node separation, and significantly higher transmission energy requirements [4–6].

Among the most promising strategies are evolutionary and bio-inspired algorithms, which have demonstrated effectiveness in addressing complex optimization problems in wireless sensor networks under dynamic conditions [7,8]. Techniques such as clustering, energy-aware routing, and fuzzy-logic-based decision mechanisms have been widely used to improve energy efficiency and network lifetime in wireless sensor networks [9].

One of the most widely known clustering protocols is LEACH (Low-Energy Adaptive Clustering Hierarchy), which has been widely used as a baseline clustering protocol for wireless sensor networks and later adapted to underwater wireless sensor networks (UWSNs) [10]. LEACH selects cluster head probabilistically and operates in two phases—setup and steady state—to reduce energy consumption and extend network lifetime. To mitigate collisions during cluster formation, S-LEACH was proposed, which divides the advertisement (ADV) phase into time slots. Additionally, C-LEACH introduces a centralized control node responsible for collecting and forwarding cluster information, reducing both collisions and energy consumption [11]. Recent studies have further investigated LEACH-based clustering mechanisms to improve energy efficiency, load balancing, and network lifetime in wireless sensor networks [12].

The issue of energy imbalance was addressed by applying an improved K-means algorithm to UWSNs [13]. This approach uses the maximum distance method to determine initial cluster centers based on node depth and local density. It selects the cluster head according to residual energy and distance metrics, thereby balancing energy consumption, extending the network lifetime, and increasing data transmission. More recent K-means-based approaches have further incorporated node location, residual energy, and sink distance into cluster-head selection to reduce energy consumption and the number of dead nodes in underwater sensor networks [14].

In the metaheuristic domain, ref. [15] proposed a clustering scheme based on Particle Swarm Optimization (PSO), which improves clustering balance by considering cluster-head load, residual energy, and transmission power to reduce energy consumption and extend network lifetime. More recent PSO-based clustering methods have further explored unequal clustering and dynamic cluster-size adjustment to balance cluster-head load and reduce overall network energy consumption in underwater sensor networks [16].

More recently, ref. [17] introduced a glowworm swarm optimization-based protocol, where cluster head are selected using a fitness function that combines residual energy, total energy, and luciferin value. This method, known as SS-GSO, achieved significant improvements in energy efficiency, cluster lifetime, and packet delivery performance.

Another promising approach is the Dragonfly Algorithm (DA), introduced by Mirjalili [18], which models separation, alignment, cohesion, attraction toward food, and distraction from enemies in a continuous search space. DA was later applied in ANC-UWSN [19] as a clustering-oriented optimization approach for underwater sensor networks, where dragonfly optimization is used to support cluster formation and routing formation. This line of work was later extended in CDFO-UWSN [20], where dragonfly optimization was combined with a multi-objective clustering formulation to improve network lifetime and energy efficiency in underwater sensor networks.

Recent advances in UWSN clustering have improved energy efficiency and packet delivery; however, several limitations remain. Many methods assume static node positions, even though underwater nodes are often affected by current-induced displacement. In addition, several optimization-based approaches rely on fixed-weight objective aggregation, which may bias the search toward particular criteria and reduce adaptability under dynamic conditions. In the case of Dragonfly-based methods applied to UWSNs, previous studies have mainly used continuous representations and weighted formulations [19,20], leaving limited exploration of binary cluster encoding and Pareto-based decision strategies.

To address these limitations, this paper proposes BMDA-UWSN, a binary multi-objective Dragonfly-based framework for cluster-head selection and clustering configuration in underwater wireless sensor networks. The contribution of the proposed method does not lie in introducing a fundamentally new swarm theory, but in reformulating the clustering problem so that candidate solutions are represented and optimized in a binary decision space suitable for UWSN clustering. In contrast to previous Dragonfly-based UWSN approaches that rely on continuous representations and fixed-weight objective aggregation, the proposed method jointly considers cluster-head selection and member assignment through binary encoding, evaluates the robustness of candidate clustering configurations under semicircular mobility conditions, and applies Pareto-based ranking with post-Pareto compromise selection to reduce dependence on fixed weights during decision making.

The proposed approach considers three optimization criteria: energy consumption, end-to-end latency, and load balance. In addition, a semicircular mobility model with angular variation of $\pm 45^{\circ}$ is incorporated to represent node oscillation caused by underwater currents within a controlled two-dimensional simulation scenario. The main contributions of this work are: (i) the adaptation of the Dragonfly-based search process to a binary decision space for UWSN clustering, (ii) the joint evaluation of clustering configurations through multi-objective optimization without relying on fixed-weight aggregation during the search stage, and (iii) the integration of a mobility-aware evaluation model to assess clustering behavior under dynamic underwater conditions. The remainder of this article is organized as follows. Section 2 presents the proposed methodology, including the network initialization procedure, the physical and communication models, the multi-objective formulation, the Dragonfly-based optimization process, and the mobility-aware evaluation simulation scenario. Section 3 describes the experimental setup and comparative evaluation. Section 4 presents the main results and their discussion. Finally, Section 5 summarizes the conclusions and outlines future work.

2. Methodology

This section presents the BMDA-UWSN methodology, which is organized into five main components, as summarized in the flowchart shown in Figure 1. First, the initialization and binary encoding stage defines node deployment, the binary representation of candidate solutions, and the initial assignment of member nodes to cluster heads. Second, the physical network models describe the communication-related mechanisms considered in the study, including energy consumption, acoustic latency, propagation loss, and load balance. Third, the semicircular mobility model represents the controlled node displacement caused by underwater currents. Fourth, the multi-objective formulation defines the optimization criteria used to evaluate candidate clustering configurations. Fifth, the optimization stage describes the binary adaptation of the Dragonfly Algorithm and the search process used to obtain the final clustering solution. The following subsections describe each component in detail.

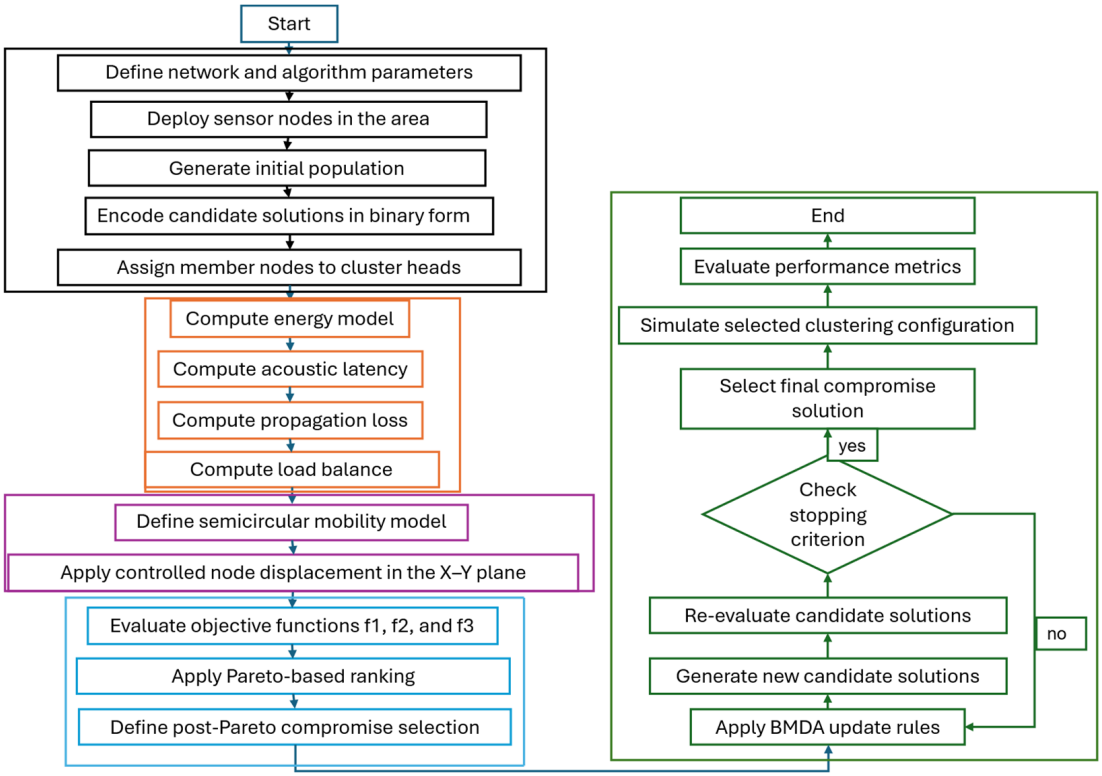


Figure 1. Flowchart of the proposed BMDA-UWSN methodology.

The diagram illustrates the main stages of the framework, including network initialization, multi-objective optimization using the binary Dragonfly algorithm, Pareto-based selection of the best global solution, and the simulation-based performance evaluation.

2.1. Initialization and Binary Encoding

A set of N sensor nodes is deployed within a two-dimensional area of 500 m × 500 m. Each node is assumed to know its Cartesian coordinates (x, y). Candidate solutions are encoded as binary vectors $\vec{v} = [b_1, b_2, \ldots, b_N]$ where each bit b_1 corresponds to node i:

$b_i = 1 \rightarrow$ node i is a cluster head (CH).

$b_i = 0 \rightarrow$ node i is a member node.

This binary representation allows the optimization process to determine the subset of nodes that will act as CHs in each candidate clustering configuration. Once the CH set is defined, each non-CH node is initially assigned to its nearest CH according to the Euclidean distance.

Initial Cluster Assignment. Each member node is associated with the nearest CH according to the Euclidean distance:

$$d = \sqrt{(x_2 - x_1)^2 + (y_2 - y_1)^2}, \quad (1)$$

where

d = Euclidean distance between two nodes.

(x_1, y_1) = coordinates of node 1.

(x_2, y_2) = coordinates of node 2.

2.2. Physical Network Models

This subsection defines the physical and communication models used to evaluate each candidate clustering configuration in BMDA-UWSN. Specifically, the framework considers

energy consumption, acoustic latency, propagation loss, and load balancing. These models provide the objective values used in the multi-objective optimization process and allow the algorithm to assess the cost of each solution under underwater communication constraints.

2.2.1. Energy Model

The energy consumption model is used in this work as a simplified network-level approximation of the communication cost associated with packet transmission and reception [21]. Its purpose is to compare candidate clustering configurations in terms of relative communication cost per round. Although this formulation does not represent the full physical behavior of underwater acoustic power consumption by itself, underwater-specific channel effects are incorporated separately in the framework through the acoustic latency, propagation-loss, and attenuation models described in Sections 2.2.2 and 2.2.3 [22]. Thus, the energy model should be interpreted as a communication-cost abstraction for network optimization rather than as a complete acoustic physical-layer power model.

$$E_{tx}(k,d) = (E_{elec} * k) + \left(E_{amp} * k * d^2\right). \tag{2}$$

Energy consumed when receiving the packet:

$$E_{rx}(k) = k * Eele, \tag{3}$$

where E_{elec} is the energy consumed by the node's electronics, E_{amp} is the energy of the transmission amplifier, d is the distance to the destination, and k is the packet size in bits. These expressions are used to estimate the transmission and reception cost associated with each communication link during intra-cluster and inter-cluster forwarding. In this way, the model provides a consistent basis for comparing candidate solutions, while underwater acoustic effects are evaluated separately through latency and propagation-loss modeling.

Intra-cluster energy (member node → CH). For each member node i assigned to its CH leader (i):

$$E_{i\to CH(i)} = \underbrace{(E_{elec} * k) + \left(E_{amp} * k * d(i,CH(i))^2\right)}_{Tx\ member} + \underbrace{k * E_{elec}}_{Rx\ CH}, \tag{4}$$

where

$E_{i\to CH(i)}$: Total energy consumed in communication between the member node i and its cluster head.

E_{elec}: Energy consumed by the node's electronics.

E_{amp}: Energy consumed by the transmission amplifier.

k: Transmitted packet size.

$d(i,CH(i))$: Euclidean distance between the node i and its cluster head.

Inter-cluster energy (backbone CH → sink). The multi-hop path from a cluster head to the sink is denoted by $P_{CH\to S}$, with links $(u \to v)$: The total energy required for inter-cluster transmission is given by

$$E_{CH\to S} = \sum_{(u\to v)\in P_{CH\to S}} \left[(E_{elec} * k) + \left(E_{amp} * k * d(u,v)^2\right)\right] + \sum_{(u\to v)\in P_{CH\to S}} [k * Eelec], \tag{5}$$

where

$E_{CH\to S}$: Total energy consumed to transmit information from a CH to the sink node through multiple hops.

$P_{CH\to S}$: Set of links ($u\to v$) forming the multi-hop path from the cluster head to the sink.

u, v = successive transmitting and receiving nodes on the path ($u \rightarrow v$).

E_{elec}: Energy consumed by the node's electronics.

E_{amp}: Energy consumed by the transmission amplifier.

k: Size of the transmitted packet.

$d(u, v)$: Distance between the transmitting node u y and the receiving node v on the multi-hop route.

Total energy per round. To quantify the total energy consumption of a candidate clustering configuration, the model considers two communication stages in each round. First, each member node transmits its packet to its assigned cluster head, while the corresponding CH consumes energy when receiving that packet. Second, only the cluster heads participate in the backbone communication toward the sink. In this stage, each backbone hop involves transmission energy at the sending CH and reception energy at the receiving CH (or at the sink, if it is the final destination). Therefore, the total energy per round is defined as the sum of intra-cluster and inter-cluster communication costs:

$$f_1(\phi) = \sum_{i \in members} [E_{tx}(k, d(i, CH(i))) + E_{rx}(k)] + \sum_{CH} \sum_{(u \rightarrow v) \in P_{CH \rightarrow S}} [E_{tx}(k, d(u, v)) + E_{rx}(k)], \quad (6)$$

where:

$f_1(\phi)$: Objective function 1, defined as represents the total energy consumed in one communication round for a given candidate solution ϕ.

$CH(i)$: Cluster head assigned to node i.

$E_{tx}(k, d)$: Energy required to transmit a packet of k bits at a distance d.

$E_{rx}(k)$: Energy required to receive a packet of k bits.

$d(i, CH(i))$: Euclidean distance between the node i and its cluster head.

$P_{CH \rightarrow S}$: Multi-hop route from cluster head to the sink.

$d(u, v)$: Distance between the transmitting node u and the receiving node v on the multi-hop route.

The first term represents intra-cluster communication, where member nodes send data to their assigned CHs. The second term represents inter-cluster backbone communication, where only CHs forward data toward the sink through multi-hop transmission.

2.2.2. Acoustic Latency

Latency in underwater acoustic communication is strongly influenced by propagation conditions and limited transmission rates [23]. For each hop between nodes n and m, the total delay is modeled as the sum of transmission delay, propagation delay, and processing delay:

Where $L_{total}(n, m)$ is the delay per hop between two nodes n and m, defined as:

$$L_{total}(n, m) = L_{tx} + L_{Prop} + L_{Proc}. \quad (7)$$

A fixed processing delay of $L_{Proc} = 5\ ms$ is assumed to represent the time required by an intermediate node to process and forward the packet.

For each link, the propagation delay is modeled as the ratio between the distance and the speed of sound in water:

$$L_{Prop} = \frac{d}{c}, \quad (8)$$

where c is the speed of sound, conventionally taken as 1500 m/s, although it can range from 1400 m/s to 1700 m/s depending on temperature, salinity, and depth [24]; d represents the distance.

The transmission delay (depends on the packet size and channel bandwidth).

$$L_{tx} = \frac{k}{R_b}, \tag{9}$$

where

k : Packet size in bits.

R_b : Transmission rate.

2.2.3. Total Propagation Loss

Total acoustic propagation loss [25], when the signal weakens when traveling underwater. It combines two effects: geometric dispersion (energy is "spread out" as the wave expands) and absorption (water attenuates more as frequency increases).

Model (in dB).

$$TLoss(d, f) = \eta * log_{10}(d) + \alpha(f) * d * 10^{-3}, \tag{10}$$

where

d: Distance between transmitter and receiver (m).

η: Represents the propagation loss exponent appropriate to the environment (10 cylindrical, 15 intermediate, 20 spherical).

$\propto (f)$: The attenuation due to absorption in dB/km, for frequency f in kHz, given by Thorp's approximation:

$$\propto (f) = \frac{0.11 f^2}{1 + f^2} + \frac{44 f^2}{4100 + f^2} + 2.75 \times 10^{-4} f^2 + 0.003. \tag{11}$$

For each link, the total path loss is first calculated:

$$U = TLoss\ (d, f). \tag{12}$$

where d is the distance between the transmitter and receiver and f is the carrier frequency. This value U reflects how much attenuation the signal suffers in the acoustic channel. Based on U, the system does not directly modify the latency but rather decides what transmission rate is sustainable for that link. In the current implementation, the total path loss is used to characterize underwater channel conditions and to determine the transmission rate that can be sustained on each link. Therefore, the propagation-loss model directly affects latency and link feasibility, while the communication energy model is treated separately as a network-level approximation of transmission and reception cost.

To do this, loss thresholds $\left\{\tau_{high}, \tau_{medium}, \tau_{low}\right\}$ are defined and associated with acceptable rate levels $\left\{R_{high}, R_{medium}, R_{low}\right\}$, which represent different modulation/coding modes of the acoustic modem.

The decision rule is expressed as:

$$R_b = \begin{cases} R_{high}, & U \leq \tau_{high} \\ R_{medium}, & \tau_{high} < U \leq \tau_{medium}, \\ R_{low}, & U \geq \tau_{low} \end{cases} \tag{13}$$

where

R_b : Transmission rate.

U : Total path loss value.

$\left\{R_{high}, R_{medium}, R_{low}\right\}$: Transmission rates available in the model.

$\{\tau_{high}, \tau_{medium}, \tau_{low}\}$: Threshold loss values in dB that define the regions of operation.

This separation allows the framework to capture the main underwater communication constraints while maintaining a computationally tractable objective evaluation during the optimization process.

The end-to-end latency of the node i is obtained by adding its intra-cluster hop and the backbone hops to the sink:

$$L_i = L_{i \to CH(i)} + \sum_{(n \to m) \in P_{CH \to S}} L_{total}(n, m), \tag{14}$$

where

L_i : End-to-end latency from node i to the sink.

$L_{i \to CH(i)}$: Latency between the member node i and its cluster head $CH(i)$.

$P_{CH \to S}$: Set of links in the multi-hop path from the cluster head $CH(i)$ to the sink.

$L_{total}(n, m)$: Total latency associated with the link between consecutive nodes n and m on the path.

To quantify the overall temporal performance of the network, it is averaged. Thus, the objective function:

$$f_2(\phi) = \frac{1}{N} \sum_{i=1}^{N} L_i, \tag{15}$$

where

$f_2(\phi)$: Objective function 2, average end-to-end latency in the network given the solution ϕ.

N: Total number of sensor nodes in the network.

L_i : End-to-end latency of the node i (defined in the previous equation).

2.2.4. Load Balancing

To evaluate the fairness of cluster formation, we quantify load balance by using the standard deviation of cluster size. A smaller standard deviation reflects a more equitable distribution of workload among cluster heads (CHs). Following [26] this can also be expressed as the standard deviation of the CH load, defined as the sum of the loads of its members after clustering. When member loads are similar, both measures are equivalent in assessing cluster uniformity.

$$\bar{s} = \frac{1}{M} \sum_{j=1}^{M} s_j. \tag{16}$$

$$f_3(\phi) = B(\phi) = \sqrt{\frac{1}{M} \sum_{j=1}^{M} (s_j - \bar{s})^2}. \tag{17}$$

where

$f_3(\phi)$: Objective function 3, load balancing measured as the standard deviation of cluster size.

$\bar{s}$: Average size of clusters in the network.

M: Total number of clusters formed in the network.

s_j: Number of nodes belonging to cluster j.

B: Standard deviation of cluster size (nodes).

2.3. Semicircular Mobility

Although the sensor nodes used in this study are physically anchored to the seabed, their design allows for restricted two-dimensional mobility induced by ocean currents and other environmental forces. This behavior is inspired by the mobility model proposed

in [27], where anchored nodes describe a spatial range of oscillation defined by a maximum angle and anchor length. In our case, this oscillation is modeled as a two-dimensional semicircular displacement of $\pm 45°$, in the X-Y plane, allowing the position of each node to vary between iterations according to:

$$\begin{aligned} x' &= x + L \cdot cos(\theta), \\ y' &= y + L \cdot sin(\theta). \end{aligned} \tag{18}$$

where $\theta \in [-45°, 45°]$ represents the oscillation angle, (x, y) represents the original coordinate, (x', y') represents the new coordinate, and L represents the maximum distance to the anchor point. Figure 2 illustrates this semicircular oscillation scheme, showing the allowed angular range for each node in each iteration. This controlled mobility model allows for the simulation of realistic effects on load balancing, latency, and connectivity, considering that the nodes do not remain static in a dynamic marine environment.

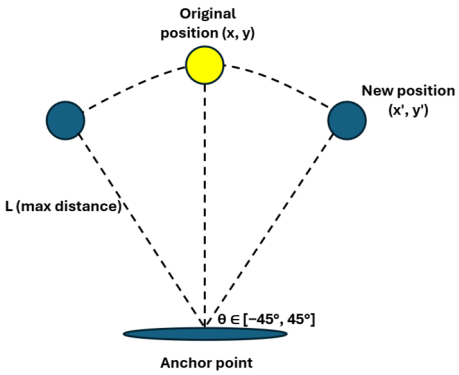


Figure 2. Scheme of permitted angular displacement for each node in each iteration.

In the current implementation, the clustering configuration is optimized before the simulation phase and is not re-optimized after node displacement. Therefore, the semicircular mobility model is used to evaluate the robustness of the optimized clustering configuration under topology perturbations, rather than to perform dynamic re-clustering at each simulation round.

2.4. Multi-Objective Formulation

We minimize the objective vector

$$F = (f_1, f_2, f_3) \qquad (to\ minimize), \tag{19}$$

where

$f_1(\phi)$—Energy per round. We add transmission and reception costs in all links used (intra- and inter-cluster), according to the first-order model (Equations (2)–(6)):

$$\begin{aligned} f_1(\phi) = &\sum_{i \in members} [E_{tx}(k, d(i, CH(i))) + E_{rx}(k)] \\ &+ \sum_{CH} \sum_{(u \to v) \in P_{CH \to S}} [E_{tx}(k, d(u, v)) + E_{rx}(k)]. \end{aligned} \tag{20}$$

$f_2(\phi)$—End-to-end latency. For each node i, we define:

$$f_2(\phi) = \frac{1}{N} \sum_{i=1}^{N} L_i. \tag{21}$$

$f_3(\phi)$ —Load balancing. We measure the uniformity of cluster sizes using standard deviation.

After constructing the non-dominated front using Pareto dominance and a diversity-preserving criterion, the final selection of a single configuration is addressed as a post-Pareto decision step. In this work, the compromise solution is chosen as the non-dominated point with minimum distance to the ideal point in the normalized objective space. Therefore, fixed-weight aggregation is avoided during the search stage, while the final selection is performed through an explicit compromise criterion applied after Pareto ranking.

Unlike weighted-sum formulations used in previous Dragonfly-based UWSN approaches, the proposed framework does not impose a fixed preference structure during the search stage. Instead, candidate solutions are ranked through Pareto dominance and diversity criteria, and a final compromise solution is selected only after constructing the non-dominated set. balance. Figure 3 shows the Pareto-front concept adopted in BMDA-UWSN. Each point corresponds to a candidate non-dominated clustering configuration evaluated in terms of the considered objectives. Figure 3 highlights the trade-off among objectives and motivates the post-Pareto selection of a representative compromise solution.

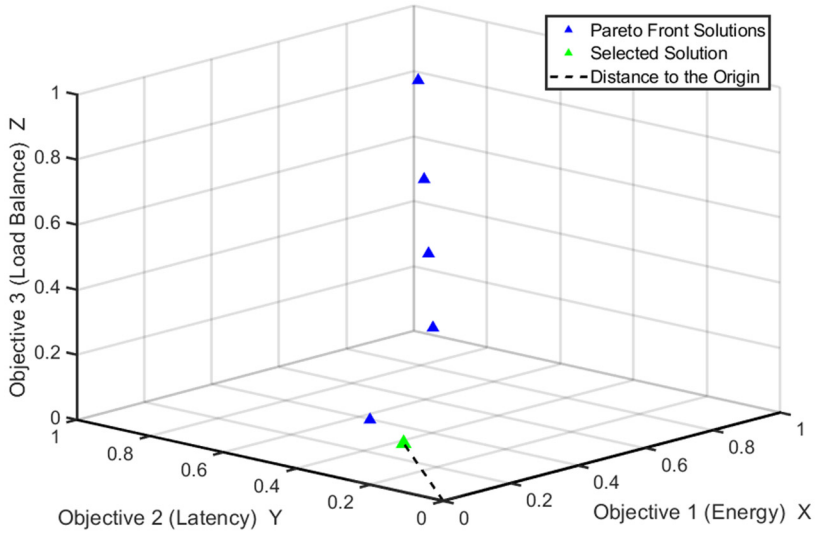


Figure 3. Pareto-front representation adopted in BMDA-UWSN.

Each point denotes a non-dominated clustering configuration evaluated according to energy consumption, end-to-end latency, and load balance.

Let f_m be a set of non-dominated solutions that constitute the Pareto front. For each solution i the objective vector is defined as $F(i) = F_1(i), F_2(i), \ldots, F_N(i)$, where $F_k(i)$ represents the value of evaluated objective k for solution i, with $k = 1, 2, \ldots, N$. Thus, each solution on the Pareto front is characterized by N values, one for each objective function of the problem. Each objective must be normalized to the interval [0, 1] using the minimum and maximum values observed within the non-dominated front $\{f_m^{min}, f_m^{max}\}$:

$$\vec{f_m}(i) = \frac{f_m - f_m^{min}}{f_m^{max} - f_m^{min}} \ (to\ minimize). \tag{22}$$

2.5. Optimization with the Dragonfly Algorithm

The Dragonfly Algorithm (DA) models two patterns observed in these insects: static swarming (around food sources) and dynamic swarming (during migration) [18]. In optimization terms, these patterns are associated, respectively, with exploitation which intensifies the search in promising solutions, and exploration which promotes the ex-

amination of new regions of the search space. This duality is particularly suitable for the UWSN clustering problem because the search process must simultaneously handle a large combinatorial space of possible cluster-head selections and clustering configurations, while also refining candidate solutions according to multiple conflicting objectives such as energy consumption, latency, and load balance. In addition, underwater communication conditions and mobility-induced topology perturbations make it desirable to preserve sufficient exploration capability before converging toward stable high-quality clustering configurations.

The choice of a binary Dragonfly-based optimizer is motivated by the nature of the UWSN clustering problem addressed in this work. Cluster-head selection and clustering configuration are inherently discrete decision processes, which makes a binary search representation more suitable than continuous formulations. In addition, UWSN clustering requires balancing multiple conflicting objectives under complex communication constraints, which demands both broad exploration of alternative configurations and refinement of promising solutions. In this context, the Dragonfly search mechanism is attractive because it explicitly balances exploration and exploitation through neighborhood interaction operators. For the proposed framework Binary Dragonfly Algorithm is adopted here as a suitable search strategy for jointly handling binary clustering decisions, multi-objective evaluation, and robustness assessment under underwater mobility conditions.

The relevance of DA in related scenarios is supported by recent work: ref. [28] reports binary variants applied to feature selection with competitive results compared to classical approaches; in [29], energy distribution networks are optimized by addressing multivariate binary variables; and ref. [30] introduces enriched search mechanisms (e.g., quantum mutations) to improve exploratory capacity without penalizing convergence. In the fields of communications networks, ref. [31] uses DA for clustering in VANET, focusing on energy consumption, while ref. [32] applies it in terrestrial WSNs to extend network life and reduce delay. This background motivates our choice of a binary/multi-objective variant adapted to the problem of joint cluster head selection and partitioning in UWSNs. DA is based on five local influences on each individual: separation (avoiding crowding), alignment (synchronizing the average direction), cohesion (attracting to the center of the neighborhood), attraction to food (moving toward promising regions), and repulsion from enemies (moving away from unfavorable regions). In our implementation, these influences are modeled as vector terms that update the status of each candidate solution.

These terms are weighted by coefficients (s, a, c, f, e), which decrease linearly over the course of iterations, and are complemented by an inertia term (w). This dynamic weighting regulates the balance between exploration (searching in new regions), exploitation (refining promising solutions), and avoiding premature convergence.

$$\Delta X_{t+1} = (sS_i + aA_i + cC_i + fF_i + eE_i) + w\Delta X_t, \tag{23}$$

where

ΔX_{t+1} : Increase in position (speed-like state) of the individual i in iteration $t + 1$.

S_i : Separation—vector that pushes i away from the center of its neighbors (avoids crowding).

A_i: Alignment—vector towards the average direction of neighbors (synchronizes movement).

C_i : Cohesion—vector towards the centroid of neighbors (keeps the group together).

F_i : Food attraction—vector towards a "desirable" position/solution (best individuals/targets).

E_i : Repulsion from the enemy—vector that moves away from "undesirable" positions (worst individuals/regions).

These pieces enable the algorithm to achieve a balance like the actual behavior of dragonflies. They move in a coordinated manner, search for food efficiently, and avoid threats, in terms of optimization, this means intelligently traversing the solution space.

After calculating the velocity vectors, the next step is to calculate the position vector:

$$X_{t+1} = X_t + \Delta X_{t+1}, \tag{24}$$

where X_{t+1} is the new position of the individual in iteration $t + 1$, X_t is the position of the individual in iteration i and ΔX_{t+1} is the position increment calculated by combining local influences and inertia (previous equation).

Although the original Dragonfly Algorithm (DA) updates positions in a continuous space, in our approach each solution is represented as a binary vector. To perform this adaptation, the continuous position update is projected onto the binary domain using a V-shaped transfer function, as proposed by [32]. This function maps the continuous variation Δx to a value in the interval [0, 1], which is interpreted as the probability of switching each bit ($0 \leftrightarrow 1$). Consequently, the resulting binary vector represents the selection of leading nodes at each iteration. The V-shaped transfer function used in this work is defined as:

$$T(\Delta x) = \left| \frac{\Delta x}{\sqrt{\Delta x^2 + 1}} \right|, \tag{25}$$

where $T(\Delta x)$ is the value of the transfer function associated with the increment Δx is in the range (0, 1) and is interpreted as the probability that the bit will change state. Δx is the continuous increment calculated in the position update stage (before the binary projection).

Binary update: to decide the state change in each bit, a random number r (0, 1) is generated.

$$X_{t+1} = \begin{cases} -x_t & r < T(\Delta X_{t+1}) \\ x_t & r \geq T(\Delta X_{t+1}) \end{cases}, \tag{26}$$

where

x_t: Binary position of the individual in the previous iteration t.

$T(\Delta X_{t+1})$: Value of the transfer function applied to the increment, interpreted as a probability in [0, 1].

That is, the bit "changes" when the randomness falls below the probability emitted by the sigmoid.

Multi-hop transmission is restricted only between the cluster head of each cluster, following the approach proposed by [33]. This strategy reduces overhead and energy consumption, as members only transmit to their leader and the calculation of energy-optimal routes using Dijkstra is performed only between leaders, thus simplifying management and extending the network life.

In underwater environments, TDMA is particularly suitable because, by assigning exclusive time slots to each node, it prevents collisions and reduces the energy consumption caused by retransmissions, as demonstrated by recent studies on energy-efficient MACs for UWSNs [4].

3. Results

This section presents the results obtained from the simulations, considering key performance metrics in UWSN: number of live nodes, end-to-end latency, residual energy, and packet delivery rate. These metrics allow us to evaluate the energy efficiency, quality of service, and robustness of the proposed algorithm.

Algorithm 1 shows the proposed pseudocode, detailing its main phases:

Algorithm 1: BMDA-UWSN

Define network parameters:
Define BMDA-UWSN parameters (dragonfly algorithm):
Create initial population (100 binary solutions):
Generate positions (x_nodes, y_nodes) randomly in the area.
Section B: BMDA-UWSN evolution (selection of cluster head)
for i = 1 to 100 each individual
    Evaluate the current population (f_1, f_2, f_3)
    Identify Food and Enemy solutions
    For each individual i in the population:
    Update velocity vector (s ∗ S + a ∗ A + c ∗ C + f ∗ F + e ∗ E) + w ∗ DeltaX
    Transfer function.
    Evaluate new population (f_1, f_2, f_3)
    Non-dominated Pareto sorting ⇒ fronts $F(i) = F_1(i), F_2(i), \ldots, F_N(i)$
    Selection by elitism (Normalized) ⇒ update Population
End, → the best global solution (BestSolution) is taken.
Section C: Initial assignment of clusters and cluster head
cluster assignment ← for each node, assign to the nearest CH
Section D: Evaluation of the best global solution
for i = 1 to 500 each individual
    Each node sends data to CH (costs ETX, ERX)
    CH sends data to Sink
    Move nodes (±45°):
    Update residual energies and live nodes
End

The simulations were implemented in MATLAB 2020 on a 9th generation Ryzen 5 system with 16 GB of RAM. The experimental scenario was defined in an area of 500 m × 500 m with 100 nodes deployed. The nodes were initially assumed to be static but subject to mobility induced by sea currents under controlled conditions. Table 1 shows the specific configuration used to perform this optimization.

Table 1. Simulation parameters used for all evaluated algorithms.

Parameters	Value
Maximum Iterations	500
Number of Nodes	100
Simulations Run	10
Area	500 m × 500 m
Frequency	25 kHz
Speed of Sound	1500 m/s

To ensure a fair and unbiased comparison, all the evaluated algorithms were tested under the same simulation environment and using identical parameter settings. Specifically, the network topology, number of nodes, deployment area, transmission range, number of iterations, and acoustic communication parameters were kept constant across all experiments. This setup guarantees that any observed performance differences are exclusively attributable to the characteristics of each algorithm rather than to variations in the simulation configuration.

Figure 4 shows the evolution of live nodes. The direct transmission scheme shows the worst performance. From iteration 58 onwards, the network has already been reduced

to 50 active nodes and barely retains 1 node at the end, showing that the absence of clustering quickly depletes energy. LEACH and C-LEACH improved substantially. However, LEACH dies out completely in iteration 400 and C-LEACH reaches 500 with 5 nodes, reflecting sustained losses in the middle of the experiment (around iteration 248 it drops to 50 active nodes).

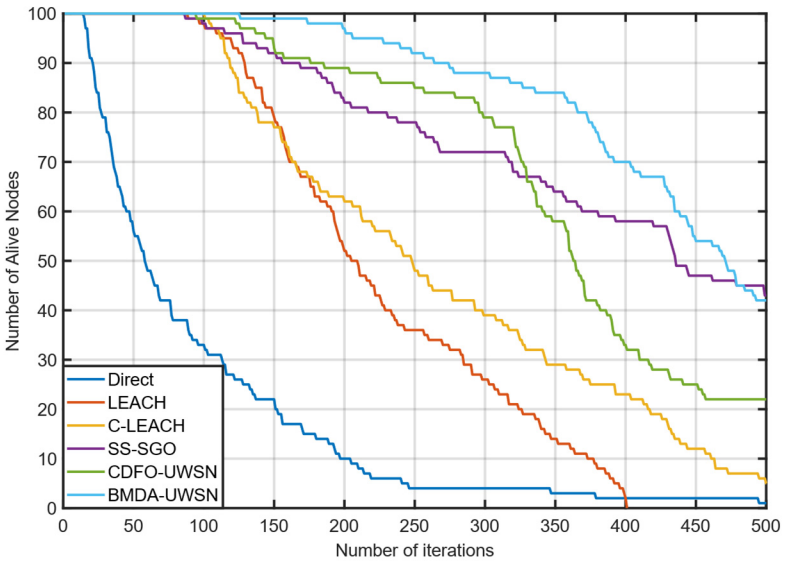


Figure 4. Alive nodes.

Among the metaheuristics, the firefly algorithm maintains a robust queue, maintaining a quantity of 43 at the end, although its curve begins to decline after iteration 300. CDFO-UWSN exhibits a broad initial plateau, with the first node deactivating at iteration 95 and remaining above SS-GSO for much of the middle of the journey, but it declines around 330 iteration and accelerates the loss of nodes, ending with 22 nodes.

The BMDA-UWSN proposal offers the best overall balance: the first node is deactivated at iteration 126, the network drops to 50 active nodes only at iteration 471, maintains 42 nodes at the end, and, on average, retains the largest fraction of the network active throughout the experiment.

The results of Table 2 show that the BMDA-UWSN proposal significantly delays the onset of node mortality. P_{50} is the percentage of iterations in which 50 nodes remain alive of the total number of iterations.

Table 2. Comparison of iterations in which nodes die.

Algorithm	Iteration First Node to Die	Iteration with 50 Live Nodes	Nodes Alive in Iteration 500	P_{50}
Direct Transmission	14	57	1	11.4%
LEACH	88	209	0	41.8%
C-LEACH	100	248	5	49.6%
SS-GSO	87	436	43	87.2%
CDFO-UWSN	94	363	22	72.6%
BMDA-UWSN	126	471	42	94.2%

This feature is especially valuable in critical applications where maximum node availability is sought during monitoring phases.

Figure 5 shows the evolution of average latency (end-to-end time node → CH → sink) of over 500 iterations for the six schemes evaluated. The comparison of the six schemes reveals two clear trends: classic protocols partially reduce latency compared to direct

transmission, but it is the bio-inspired approaches that make a substantial difference in the stability of the accumulated delay.

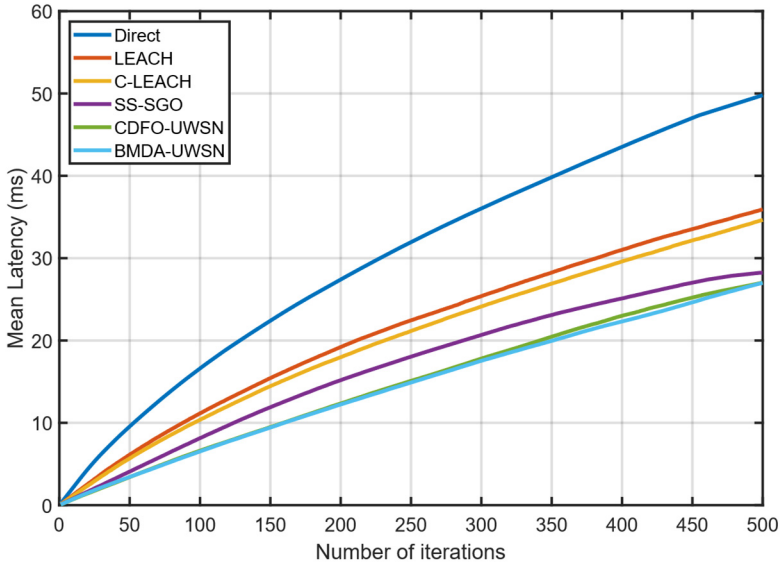


Figure 5. Latency.

As shown in Table 3, the Direct scheme achieves an average of 30.04 s and an extreme value of 49.79 s, reflecting accelerated latency growth throughout the process. In contrast, LEACH and C-LEACH moderate this behavior with averages around 21 s and final delays of 35 s; however, their reduction compared to the base scheme (≈30%) is insufficient in scenarios where precise synchronization is critical.

Table 3. Initial and final latency.

Algorithm	Arithmetic Means	Latency (Iter. 500)	Reduction vs. Direct *
Direct transmission	30.04 s	49.79 s	—
LEACH	21.11 s	35.88 s	28%
C-LEACH	20.10 s	34.70 s	30%
SS-GSO	16.79 s	28.22 s	43%
CDFO-UWSN	14.73 s	27.99 s	44%
BMDA-UWSN	14.48 s	27.00 s	46%

* Reduction calculated with respect to the final metric for direct transmission.

For their part, metaheuristic algorithms not only reduce average latency but also achieve a much more controlled closure. SS-GSO maintains an average of 16.79 s and a final value of 28.22 s, achieving an improvement of 43%. The CDFO-UWSN algorithm drops even further to 14.73 s and concludes with 27.99 s, confirming that dynamic route construction allows the network to remain less congested.

Finally, the BMDA-UWSN proposal exhibits the best consistency: with an average of 14.48 s and a final delay of 27.00 s, it achieves the greatest reduction compared to the direct model (46%). Beyond the specific values, it is noteworthy that its growth curve is more progressive and less abrupt, which means that delays accumulate slowly, and the network preserves its efficient transmission capacity for longer.

In practical terms, this stability is as important as the absolute reduction in seconds, as it ensures that events and packets arrive in a more synchronized and reliable manner, reinforcing the robustness of the underwater network.

Figure 6 compares the cumulative number of packets correctly received at the sink with over 500 iterations for the six schemes evaluated.

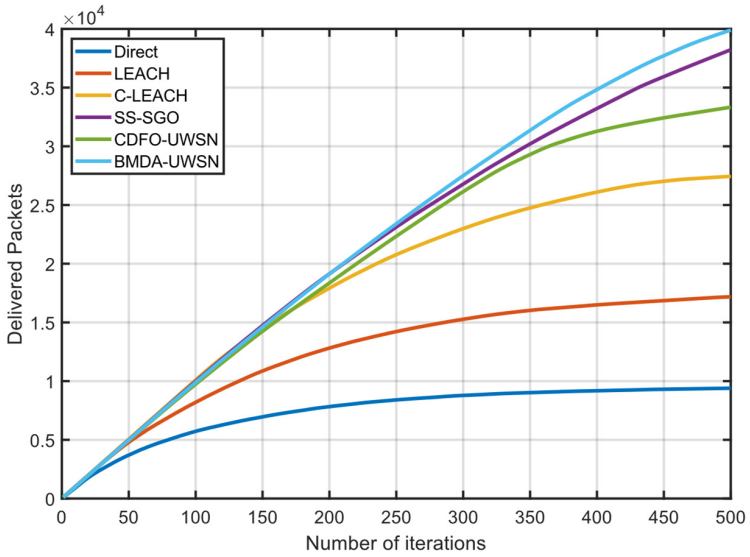


Figure 6. Packet delivery.

As shown in Table 4, there are significant differences between classical and bio-inspired algorithms in terms of packet delivery capacity across the network.

Table 4. Number of packets delivered.

Algorithm	Packets Delivered (Iter. 250)	Packets Delivered (Iter. 500)	Improvement vs. Direct-Tx Transmission *
Direct transmission	8344	9393	—
LEACH	14,220	17,180	+83%
C-LEACH	20,770	27,440	+192%
SS-GSO	23,130	38,180	+306%
CDFO-UWSN	22,340	33,330	+255%
BMDA-UWSN	23,400	39,900	+325%

* Relative to the final Direct Transmission data.

The Direct Transmission scheme offers the lowest values, reaching only 8344 packets in iteration 250 and a total of 9393 in iteration 500. This result reflects its fundamental limitation: rapid energy depletion of the nodes generates inefficient routes and accumulated information losses.

In contrast, LEACH and C-LEACH achieve significant improvements thanks to clustering. LEACH reaches 17,180 packets at the end of the experiment (+83% vs. direct), while C-LEACH surpasses it with 27,440 packets (+192%). However, both protocols have a more moderate slope, suggesting some loss of efficiency in prolonged scenarios.

Metaheuristic algorithms stand out significantly. SS-GSO achieves 38,180 packets at the end, representing a 306% increase over the base model. Similarly, CDFO-UWSN delivers 33,330 packets (+255%), demonstrating that dynamic route optimization favors a more sustained flow of information.

Finally, the BMDA-UWSN proposal achieves the best overall performance: 23,400 packets halfway through the process and 39,900 at the end, with a 325% improvement over direct transmission. Beyond this absolute value, the stability of its progression stands out: it maintains continuous growth throughout the experiment, avoiding the intermediate stagnations observed in LEACH and C-LEACH.

In practical terms, this behavior means that the proposal not only extends the network's useful life, but also maximizes data collection efficiency, ensuring that most of the information generated by the nodes effectively reaches the sink.

Figure 7 shows the comparative evaluation of residual energy (all curves start at 500 J per node).

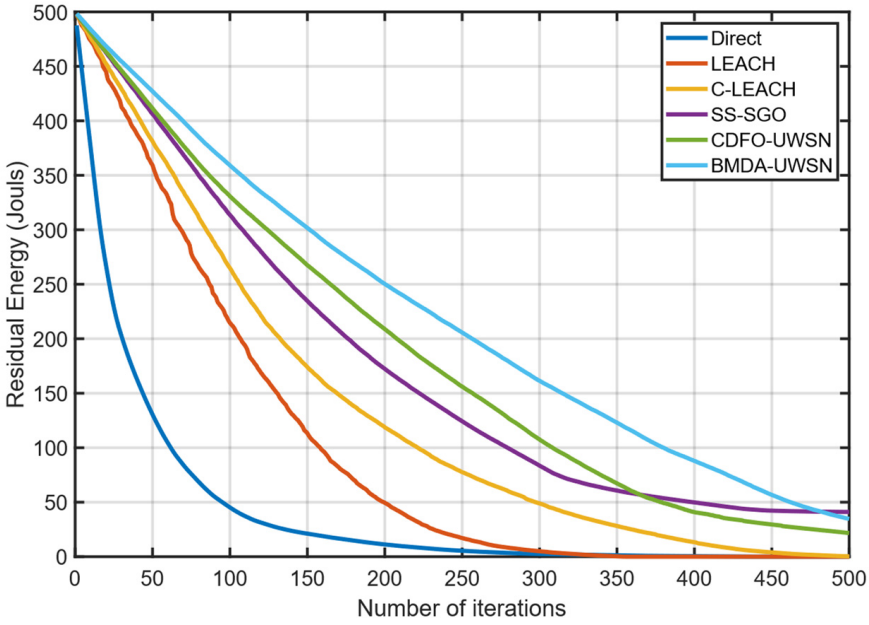


Figure 7. Residual energy.

Table 5 shows the results of residual energy development, the first phase, all algorithms still show high energy levels. However, BMDA-UWSN retains 427 J, the highest value among all, which is ≈3 times more than Direct Transmission (130.5 J) and an additional 4% over CDFO-UWSN (411.4 J). This indicates that from the outset, the proposal manages consumption more efficiently, avoiding early energy losses.

Table 5. Residual energy development.

Algorithm	Energy at Iter. 50 (J)	Energy at Iter. 250 (J)	Energy at Iter. 500 (J)
Direct transmission	130.5	5.44	0
LEACH	359.3	17.13	0
C-LEACH	381.2	77.59	0.2
SS-GSO	406.2	124.3	41.04
CDFO-UWSN	411.4	156.1	21.71
BMDA-UWSN	427	205.7	34.73

The difference widens significantly: BMDA-UWSN maintains 205.7 J, while CDFO-UWSN and SS-GSO register 156.1 J and 124.3 J, respectively. In contrast, classic protocols such as LEACH barely retain 17.13 J and Direct Transmission only 5.44 J. This means that, halfway through the experiment, the proposal retains ≈38 times more energy than Direct Transmission and ≈12 times more than LEACH.

In the critical phase, when the network begins to run out of power, BMDA-UWSN continues to show robust performance with 34.73 J of residual energy, compared to 41.04 J for SS-GSO and 21.71 J for CDFO-UWSN. The classic protocols are already completely depleted (0–0.2 J). Although SS-GSO retains a slight advantage in absolute energy, the proposal remains competitive, clearly outperforming CDFO-UWSN (+60%) and tripling the final energy of C-LEACH.

The analysis reveals that BMDA-UWSN is the most efficient protocol in the early and intermediate stages, ensuring balanced consumption and extending the network's useful life. In the final stage, it remains among the best, consolidating a sustained energy-saving

strategy that far exceeds traditional schemes and remains competitive with bio-inspired algorithms such as SS-GSO.

4. Discussion

The results obtained show that classic protocols such as LEACH and C-LEACH, improve upon Direct Transmission. However, their performance is limited in prolonged scenarios with high energy demand. These protocols demonstrate early node exhaustion and accelerate residual energy loss, which compromises monitoring continuity. This is consistent with the literature, which recognizes that fixed clustering schemes tend to lose efficiency as the experiment progresses.

In contrast, the bio-inspired algorithms analyzed—SS-GSO, CDFO-UWSN, and BMDA-UWSN—confirm the ability of metaheuristics to better balance energy consumption, maintain more stable hierarchical routes, and reduce end-to-end latency. The SS-GSO algorithm shows an advantage in final residual energy, reflecting its strength in dynamic load redistribution. However, the performance of BMDA-UWSN stands out for its overall consistency: it delays the death of the first node longer, maintains a stable level of latency, and achieves the highest cumulative packet delivery. This consistency across several metrics suggests that the combination of binary multi-objective search and mobility-aware evaluation favors more resilient and sustainable clustering behavior under the evaluated conditions.

A direct comparison with CDFO-UWSN reinforces this point: although both employ strategies derived from the Dragonfly Algorithm, the replacement of fixed-weight aggregation during the search stage with Pareto-based ranking may help BMDA-UWSN reduce premature bias toward a single objective and maintain a more balanced trade-off between energy, delay, and transmission efficiency. This results in not only being a longer-lasting network, but also one that is more reliable in terms of the quality of the data collected.

Beyond the numerical comparison, these trends can be interpreted considering the methodological design of BMDA-UWSN.

A deeper interpretation of the observed performance of BMDA-UWSN suggests that the improvement is likely associated with the interaction of several methodological components rather than with a single isolated factor. First, the binary representation allows candidate solutions to be expressed directly in a decision space aligned with the discrete nature of cluster-head selection. This reduces the mismatch between the clustering problem and the search representation, which may favor more coherent candidate configurations during optimization.

Second, the Pareto-based multi-objective strategy avoids imposing fixed objective weights during the search stage. Instead of privileging a predefined combination of energy, latency, and load balance, the search process preserves multiple non-dominated alternatives and defers the final choice to a post-Pareto compromise step. Under the evaluated simulation conditions, this strategy may help preserve solution diversity and produce more balanced clustering configurations than approaches based on fixed-weight aggregation.

Third, the Dragonfly-based search process contributes through its balance between exploration and exploitation. Exploration allows the algorithm to examine alternative clustering arrangements, while exploitation refines promising candidate solutions. This behavior is particularly relevant in UWSN clustering, where the search space is combinatorial and the objectives are mutually conflicting. In this sense, the observed improvements are plausibly related to the combined effect of binary encoding, Pareto-based ranking, and Dragonfly search dynamics.

At the same time, the mobility model used in this work should be interpreted as part of the evaluation stage rather than as a dynamic re-optimization mechanism. Therefore, the results under node displacement are better understood as evidence of robustness

of the optimized clustering configuration under controlled topology perturbations. A formal component-wise analysis isolating the individual contribution of binary encoding, Pareto-based decision, and Dragonfly search dynamics were not included in the current manuscript. This remains an important direction for future work.

5. Conclusions

This paper presented BMDA-UWSN, a binary multi-objective Dragonfly-based framework for clustering in underwater wireless sensor networks. The proposed method reformulates the clustering problem in a binary decision space and evaluates candidate solutions using three criteria: energy consumption, end-to-end latency, and load balance. In contrast to fixed-weight approaches, BMDA-UWSN applies Pareto-based ranking during the search stage and a post-Pareto compromise selection to choose a representative final solution.

Under the evaluated simulation conditions, BMDA-UWSN achieved better overall performance than the compared methods in terms of network lifetime, packet delivery, latency, and residual energy. In particular, the proposed framework delayed the first-node-dead event, improved packet delivery, and reduced latency with respect to the reference methods considered in this study. These results indicate that BMDA-UWSN is a competitive clustering alternative for underwater monitoring scenarios when assessed under controlled node mobility conditions.

The main contribution of this work lies in the problem-specific reformulation of Dragonfly-based clustering for UWSNs. More specifically, the method combines binary encoding for clustering configuration, a Pareto-based multi-objective search strategy without fixed-weight aggregation during the search stage, post-Pareto compromise selection based on distance to the ideal point, and robustness assessment under semicircular node displacement. In this sense, the contribution is not claimed as a fundamentally new swarm theory, but as a clustering-oriented adaptation of the Dragonfly search process to the constraints of underwater wireless sensor networks. A more comprehensive quantitative assessment of Pareto-front quality was not included in the current study and may be considered in future work to further analyze the convergence and distribution of the obtained non-dominated solutions.

Therefore, future work should consider tighter coupling between acoustic propagation and communication power, adaptive re-clustering under node displacement, broader validation under more representative underwater conditions, including three-dimensional mobility and more complex acoustic channel assumptions, and a formal analysis of the individual contribution of binary encoding.

Author Contributions: Conceptualization, E.V. and A.M.; methodology, E.V., A.M. and L.A.G.; software, E.V., A.M. and A.R.; validation, E.V., G.R. and L.A.G.; formal analysis, E.V., A.M. and G.R.; investigation, A.M. and E.V.; resources, L.A.G. and A.R.; data curation, E.V.; writing—original draft preparation, E.V. and A.M.; writing—review and editing, A.R., L.A.G. and G.R.; visualization, A.M.; supervision, A.M. All authors have read and agreed to the published version of the manuscript.

Funding: This research received no external funding.

Data Availability Statement: The original contributions presented in this study are included in the article. Further inquiries can be directed to the corresponding author.

Acknowledgments: This work was partially supported by the Universidad Autónoma de Tamaulipas under Grant Fortalecimiento del Grupo de Investigación en Electrónica de la Unidad Académica Multidisciplinaria Reynosa Rodhe, PEI2018-UAT-2022.

Conflicts of Interest: The authors declare no conflicts of interest.

References

1. Ahanian, I.; Mahdi, H.A.; Abd, H.J. Overview of Optical Wireless Networks Technology Underwater. *J. Univ. Babylon Eng. Sci.* **2024**, *32*, 127–139.
2. Qu, Z.; Lai, M. A Review on Electromagnetic, Acoustic, and New Emerging Technologies for Submarine Communication. *IEEE Access* **2024**, *12*, 12110–12125. [CrossRef]
3. Hasan, W.K.; Ahmad, I.; Habibi, D.; Phung, Q.V.; Al-Fawa'reh, M.; Islam, K.Y.; Zaheer, R.; Khaled, H. A Survey on Energy Efficient Medium Access Control for Acoustic Wireless Communication Networks in Underwater Environments. *J. Netw. Comput. Appl.* **2025**, *235*, 104079. [CrossRef]
4. Akyildiz, I.F.; Pompili, D.; Melodia, T. Challenges for Efficient Communication in Underwater Acoustic Sensor Networks. *ACM SIGBED Rev.* **2004**, *1*, 3–8. [CrossRef]
5. Ayaz, M.; Ammad-Uddin, M.; Sharif, Z.; Hijji, M.; Mansour, A. A Hybrid Data Collection Scheme to Achieve Load Balancing for Underwater Sensor Networks. *J. King Saud Univ. Comput. Inf. Sci.* **2023**, *35*, 74–86. [CrossRef]
6. Marco, K.; Goyal, S.; Kaur, R. A Review of Underwater Wireless Sensor Networks Deployment Techniques and Challenges. *Babylon. J. Netw.* **2024**, *2024*, 111–121. [CrossRef]
7. Sheeja, R.; Iqbal, M.M.; Sivasankar, C. Multi-Objective-Derived Energy Efficient Routing in Wireless Sensor Network Using Adaptive Black Hole-Tuna Swarm Optimization Strategy. *Ad. Hoc. Netw.* **2023**, *144*, 103140. [CrossRef]
8. Faheem, M.; Ngadi, M.A.; Gungor, V.C. Energy Efficient Multi-Objective Evolutionary Routing Scheme for Reliable Data Gathering in Internet of Underwater Acoustic Sensor Networks. *Ad. Hoc. Netw.* **2019**, *93*, 101912. [CrossRef]
9. Zhang, H.; Zhang, M.; Qin, T.; Wei, W.; Fan, Y.; Yang, J. An Energy Consumption Optimization Strategy for Wireless Sensor Networks via Multi-Objective Algorithm. *J. King Saud Univ. Comput. Inf. Sci.* **2024**, *36*, 101919. [CrossRef]
10. Mansouri, D.; Ioualalen, M. Adapting LEACH Algorithm for Underwater Wireless Sensor Networks. In Proceedings of the Eleventh International Multi-Conference on Computing in the Global Information Technology, Barcelona, Spain, 13–17 November 2016; pp. 36–41.
11. Li, Y.; Wang, Y.; Ju, Y.; He, R. Energy Efficient Cluster Formulation Protocols in Clustered Underwater Acoustic Sensor Networks. In Proceedings of the 2014 7th International Conference on Biomedical Engineering and Informatics, Dalian, China, 14–16 October 2014; pp. 923–928.
12. Ramya, R.; Srinivasan, S.; Vasudevan, K.; Poonguzhali, I. Energy Efficient Enhanced LEACH Protocol for IoT Based Applications in Wireless Sensor Networks. In Proceedings of the 2022 International Conference on Inventive Computation Technologies (ICICT), Lalitpur, Nepal, 20–22 July 2022; pp. 953–961.
13. Zhang, Y.; Sun, H.; Yu, J. Clustered Routing Protocol Based on Improved K-Means Algorithm for Underwater Wireless Sensor Networks. In Proceedings of the 2015 IEEE International Conference on Cyber Technology in Automation, Control, and Intelligent Systems (CYBER), Shenyang, China, 8–12 June 2015; pp. 1304–1309.
14. Li, L.; Qiu, Y.; Xu, J. A K-Means Clustered Routing Algorithm with Location and Energy Awareness for Underwater Wireless Sensor Networks. *Photonics* **2022**, *9*, 282. [CrossRef]
15. Li, P.; Wang, S.; Zhang, H.; Zhang, E. Improved Particle Swarm Optimization Algorithm of Clustering in Underwater Acoustic Sensor Networks. In Proceedings of the OCEANS 2017—Aberdeen, Aberdeen, UK, 19–22 June 2017; pp. 1–7.
16. Hou, R.; Fu, J.; Dong, M.; Ota, K.; Zeng, D. An Unequal Clustering Method Based on Particle Swarm Optimization in Underwater Acoustic Sensor Networks. *IEEE Internet Things J.* **2022**, *9*, 25027–25036. [CrossRef]
17. Bharany, S.; Sharma, S.; Alsharabi, N.; Tag Eldin, E.; Ghamry, N.A. Energy-Efficient Clustering Protocol for Underwater Wireless Sensor Networks Using Optimized Glowworm Swarm Optimization. *Front. Mar. Sci.* **2023**, *10*, 1117787. [CrossRef]
18. Mirjalili, S. Dragonfly Algorithm: A New Meta-Heuristic Optimization Technique for Solving Single-Objective, Discrete, and Multi-Objective Problems. *Neural Comput. Appl.* **2016**, *27*, 1053–1073. [CrossRef]
19. Khan, M.F.; Bibi, M.; Aadil, F.; Lee, J.W. Adaptive Node Clustering for Underwater Sensor Networks. *Sensors* **2021**, *21*, 4514. [CrossRef]
20. Kaveripakam, S.; Chinthaginjala, R. Clustering-Based Dragonfly Optimization Algorithm for Underwater Wireless Sensor Networks. *Alex. Eng. J.* **2023**, *81*, 580–598. [CrossRef]
21. Kaveripakam, S.; Chinthaginjala, R. Energy Balanced Reliable and Effective Clustering for Underwater Wireless Sensor Networks. *Alex. Eng. J.* **2023**, *77*, 41–62. [CrossRef]
22. Wu, Z.; Tian, C.; Jiang, H.; Liu, W. Minimum-Latency Aggregation Scheduling in Underwater Wireless Sensor Networks. In *IEEE International Conference on Communications (ICC), Kyoto, Japan, 5–9 June 2011*; IEEE Communications Society: New York, NY, USA, 2011.
23. Kularia, Y.; Kohli, S.; Bhattacharya, P.P. Analysis of Acoustic Channel Characteristics for Underwater Wireless Sensor Networks. *Int. J. Comput. Sci. Inf. Technol. Control Eng.* **2016**, *3*, 11–24. [CrossRef]
24. Ahmad, I.; Rahman, T.; Zeb, A.; Khan, I.; Ben Othman, M.T.; Hamam, H. Cooperative Energy-Efficient Routing Protocol for Underwater Wireless Sensor Networks. *Sensors* **2022**, *22*, 6945. [CrossRef] [PubMed]

25. Sreenivasamurthy, S.; Obraczka, K. Clustering for Load Balancing and Energy Efficiency in IoT Applications. In Proceedings of the Proceedings—26th IEEE International Symposium on Modeling, Analysis and Simulation of Computer and Telecommunication Systems, MASCOTS 2018, Milwaukee, WI, USA, 25–28 September 2018; pp. 319–332.
26. Guang, X.; Liu, C.; Qu, W.; Zhao, Z. Dynamic Data Collection Algorithm Based on Mobile Edge Computing in Underwater Internet of Things. *J. Cloud Comput.* **2023**, *12*, 46. [CrossRef]
27. Hammouri, A.I.; Mafarja, M.; Al-Betar, M.A.; Awadallah, M.A.; Abu-Doush, I. An Improved Dragonfly Algorithm for Feature Selection. *Knowl. Based Syst.* **2020**, *203*, 106131. [CrossRef]
28. Tian, H.; Yuan, C.; Li, K. Robust Optimization of the Continuous Annealing Process Based on a Novel Multi-Objective Dragonfly Algorithm. *Eng. Appl. Artif. Intell.* **2021**, *106*, 104448. [CrossRef]
29. Yu, C.; Cai, Z.; Ye, X.; Wang, M.; Zhao, X.; Liang, G.; Chen, H.; Li, C. Quantum-like Mutation-Induced Dragonfly-Inspired Optimization Approach. *Math. Comput. Simul.* **2020**, *178*, 259–289. [CrossRef]
30. Elhoseny, M.; Shankar, K. Energy Efficient Optimal Routing for Communication in VANETs via Clustering Model. In *Emerging Technologies for Connected Internet of Vehicles and Intelligent Transportation System Networks*; Springer: Cham, Switzerland, 2020; pp. 1–14.
31. Vinodhini, R.; Gomathy, C. A Hybrid Approach for Energy Efficient Routing in WSN: Using DA and GSO Algorithms. In *Inventive Computation Technologies*; Springer: Cham, Switzerland, 2020; pp. 506–522.
32. Mirjalili, S.; Lewis, A. S-Shaped versus V-Shaped Transfer Functions for Binary Particle Swarm Optimization. *Swarm Evol. Comput.* **2013**, *9*, 1–14. [CrossRef]
33. Razzaq, M.; Shin, S. Fuzzy-Logic Dijkstra-Based Energy-Efficient Algorithm for Data Transmission in WSNs. *Sensors* **2019**, *19*, 1040. [CrossRef]

Disclaimer/Publisher's Note: The statements, opinions and data contained in all publications are solely those of the individual author(s) and contributor(s) and not of MDPI and/or the editor(s). MDPI and/or the editor(s) disclaim responsibility for any injury to people or property resulting from any ideas, methods, instructions or products referred to in the content.